Journal of Solid State Chemistry **155,** 138–142 (2000)
doi:10.1006/jssc.2000.8914, available online at http://www.idealibrary.com on IDEAL®

True Tolerance Factor Effects in $Ln^{3+}_{1.85}M^{2+}_{0.15}CuO_4$ Superconductors

J. A. McAllister, S. Davies, and J. P. Attfield

Department of Chemistry, University of Cambridge, Lensfield Road, Cambridge CB2 1EW, United Kingdom; and the Interdisciplinary Research Centre in Superconductivity, University of Cambridge, Madingley Road, Cambridge CB3 0HE, United Kingdom

Received June 15, 2000; in revised form August 1, 2000; accepted August 2, 2000

DEDICATED TO PROFESSOR J. M. HONIG

A series of seven $Ln^{3+}_{1.85}M^{2+}_{0.15}CuO_4$ samples has been prepared in which mixtures of Ln = La and Nd and M = Ca, Sr, and Ba are used to increase the average radius from 1.180 to 1.223 Å (equivalent to an increase of tolerance factor from 0.856 to 0.871) while the size variance is fixed at a constant value of $\sigma^2 = 0.0020$ Å^2. X-ray powder diffraction is used to study structural changes, and ac magnetic susceptibility, electrical resistivity, and thermoelectric power measurements show the variation of physical properties as a true function of the tolerance factor.

INTRODUCTION

The superconducting A_2CuO_4 cuprates are intergrowths of CuO_2 copper oxide planes and insulating double AO layers (A is a mixture of Ln^{3+} rare-earth and M^{2+} alkaline earth cations). For the La_2CuO_4 type structure to be stable there should be sufficient matching between the bond lengths in each layer. This is traditionally measured by the perovskite tolerance factor, $t = (\langle r_A \rangle + r_o)/\sqrt{2}(r_{Cu} + r_o)$ where $\langle r_A \rangle$ is the mean A cation radius and r_{Cu} and r_o are the copper and oxide ion radii. The mismatch between La–O and Cu–O bonds is large so that $t < 1$, placing the Cu–O bonds under compression and La–O under tension. This can be alleviated through tilting of the CuO_6 octahedra or by substitution with a larger cation. Doping with an alkaline earth-metal cation has the added effect of removing an antibonding electron from the Cu–O bond. If La is replaced by a smaller ion the tolerance factor is reduced further and eventually a transition to the T′ (Nd_2CuO_4 type) structure occurs (1). The physical behavior of the single-layer high T_c cuprates is also strongly dependent on the properties of the insulating layer between the copper oxide planes (2). By altering the A site composition in T-type $(Ln^{3+}_{1-x}M^{2+}_x)_2CuO_4$ the superconducting properties, as well as structural transitions, can be tuned (3, 4).

Recently it has been shown that the cation size variance $\sigma^2 (= \langle r_A^2 \rangle - \langle r_A \rangle^2)$ is also important in controlling the behavior of $(Ln^{3+}_{1-x}M^{2+}_x)_2CuO_4$ cuprates (5). If the doping level is fixed (at the optimum $x = 0.075$ value) and $\langle r_A \rangle$ is held constant, then the superconducting critical temperature T_c decreases linearly with σ^2 while the structural transition from the high temperature tetragonal (HTT, $I4/mmm$ symmetry) to the low temperature orthorhombic (LTO1, *Abma* symmetry) structure increases linearly (6). Systematic changes in the carrier densities in the normal and superconducting states are also evidenced from magnetic and transport measurements (6, 7).

Previous studies of the A cation size (tolerance factor) effects in $(Ln^{3+}_{1-x}M^{2+}_x)_2CuO_4$ superconductors did not allow for the size variance effect, and so we have undertaken this study of a series of optimally doped ($x = 0.075$) materials in which σ^2 is also fixed at a convenient value (0.002 Å^2) in order to demonstrate the true tolerance factor dependence of the structural and superconducting properties.

EXPERIMENTAL

A series of seven samples were prepared, each with $\sigma^2 = 0.002$ Å^2 and covering a range of $1.180 \leq \langle r_A \rangle \leq 1.223$ Å (calculated using standard nine-coordinate ionic radii (8)). Sample compositions are given in Table 1. Appropriate amounts of La_2O_3, Nd_2O_3, $CaCO_3$, $SrCO_3$, $BaCO_3$, and CuO were ground together, pressed into pellets, and heated at 950°C for 24 h to achieve decarbonation. The samples were reground and heated at 1050°C for 200 h with several intermediate regrindings. After the final heating, the pellets were annealed in flowing oxygen at 400°C for 100 h.

The samples were characterized by powder X-ray diffraction scans, collected over 8 h on a STOE STADI P diffractometer from $20 \leq 2\theta \leq 90^\circ$ using monochromated Cu$K\alpha_1$ radiation with a step size of 0.01°. Rietveld fits were performed using the GSAS package (9) to determine cell parameters and phase fractions (Tables 1 and 2).

Only samples 4–7 were found to contain a single La_2CuO_4 type phase and these were further characterized by thermogravimetric analysis from 20 to 800°C under

0022-4596/00 $35.00

TABLE 1
A Site Composition, Average Radius $\langle r_A \rangle$, Tolerance Factor (t), and Phase Fractions from X-ray Diffraction Analysis for Seven A_2CuO_4 Samples

Sample no.	A site composition	$\langle r_A \rangle$ (Å)	t	Phase fractions (%)			
				T′	$La_2CaCu_2O_6$	T (LTO1)	T (HTT)
1	$La_{0.185}Nd_{0.740}Ca_{0.050}Sr_{0.008}Ba_{0.017}$	1.180	0.856	86.4(2)	13.6(2)	0	0
2	$La_{0.369}Nd_{0.556}Ca_{0.045}Sr_{0.016}Ba_{0.014}$	1.190	0.860	60.0(1)	15.0(1)	25.0(1)	0
3	$La_{0.490}Nd_{0.435}Ca_{0.010}Sr_{0.057}Ba_{0.008}$	1.200	0.863	14.7(4)	0	85.3(4)	0
4	$La_{0.640}Nd_{0.285}Ca_{0.035}Sr_{0.024}Ba_{0.016}$	1.206	0.865	0	0	100	0
5	$La_{0.704}Nd_{0.221}Ca_{0.013}Sr_{0.047}Ba_{0.015}$	1.212	0.867	0	0	100	0
6	$La_{0.797}Nd_{0.128}Ca_{0.010}Sr_{0.046}Ba_{0.019}$	1.218	0.869	0	0	100	0
7	$La_{0.925}Ca_{0.037}Sr_{0.008}Ba_{0.030}$	1.223	0.871	0	0	0	100

H_2/N_2, and the following physical measurements. AC susceptibilities were recorded for powdered samples in a field of 1 G, with frequency 333 Hz, in the temperature range 4.2–50 K to determine T_c and the diamagnetic fractions. Four probe resistivity measurements were made on sintered bars in the temperature range 8–300 K, with a measuring current of 100 μA. The room-temperature thermoelectric power $S(290)$ was determined using the apparatus developed by Obertelli *et al.* (10) and the corresponding hole concentration was estimated from standard data (11). Results of these measurements are shown in Table 3.

RESULTS AND DISCUSSION

a. Structure Analysis

The major phases found from the powder X-ray diffraction analyses of the seven samples are shown in Table 1, although small proportions (< 5%) of additional phases may not be observed. The analyses reveal changes in the A_2CuO_4 structure type and the phase assemblage as $\langle r_A \rangle$ increases from 1.18 to 1.223 Å. The structure type changes from T′ (Nd_2CuO_4 type) to T (La_2CuO_4 type), as is well known from previous studies, e.g., Ref. 1. In the T′ structure, the CuO_2 planes are under tension and so can be electron doped giving the *n*-type superconductors such as $Nd_{2-x}Ce_xCuO_4$ (12,13). However, they are not amenable to *p*-type doping, so that in samples 1 and 2 the M^{2+} cations segregate into a secondary $La_2CaCu_2O_6$-type phase (14, 15), which can accommodate Sr on Ca sites and Ba on the La sites. Assuming the latter cation distribution allows the phase segregation in sample 1 to be written as

$$\begin{aligned}(La_{0.19}Nd_{0.74}Ca_{0.05}Sr_{0.01}Ba_{0.02})_2CuO_4 \\ \rightarrow 0.76(Nd_{0.97}La_{0.03})_2CuO_4 \\ + 0.12(La_{0.83}Ba_{0.17})_2(Ca_{0.83}Sr_{0.17})Cu_2O_{6-x} \\ + 0.07La_2O_3.\end{aligned}$$

The expected Nd_2CuO_4-type/$La_2CaCu_2O_6$-type ratio of $0.76/0.12 = 6.33$ compares extremely well with the observed ratio (Table 1) of $86.4/13.6 = 6.35$, although the additional La_2O_3 is not observed and this may have formed a poorly crystalline carbonate or hydroxide. The presence of the secondary $La_2CaCu_2O_6$-type phase shows that σ^2 is not a good functional for the $\langle r_A \rangle < 1.20$ Å samples in this study, as the observed phases depend upon the proportions of the A-type cations, and not just the statistics of the overall A cation distribution.

TABLE 2
Structure Type, Lattice Parameters, Cell Volume (×0.5 for LTO1 Phases), and Orthorhombicity (o) for the Majority A_2CuO_4 Phases in Samples 1–7

Sample no.	Structure type	a (Å)	b (Å)	c (Å)	V (Å^3)	o
1	T′	3.95826(9)	—	12.2481(3)	191.90(1)	0
2	T′	3.96271(5)	—	12.2822(3)	192.87(1)	0
3	T(LTO1)	5.3659(1)	5.3129(1)	13.0686(2)	186.29(1)	0.00992
4	T(LTO1)	5.3530(2)	5.3120(2)	13.0772(6)	185.93(2)	0.00768
5	T(LTO1)	5.3610(2)	5.3314(2)	13.1482(6)	187.90(2)	0.00554
6	T(LTO1)	5.3374(2)	5.3232(2)	13.1609(5)	186.97(1)	0.00267
7	T(HTT)	3.7857(1)	—	13.2272(2)	189.56(1)	0

The change from T′ to T-type structure is seen in samples 2 and 3 which contain both phases and have tolerance factors $0.860 \leq t \leq 0.863$. A study by Manthiram and Goodenough (1) of the tolerance factor effects on the structures of undoped $La_{2-y}Nd_yCuO_4$ solid solutions found the T′ to T transition at a slightly lower tolerance factor ($t \leq 0.859$), although in this series there is also a varying σ^2 of magnitude $0.0007 \cdot y \cdot (2 - y)$ Å^2.

The T phases in samples 2–6 were found to have the LTO1 structure, but 7 has the undistorted HTT arrangement. Rietveld fits were used to refine the lattice parameters (Table 2) and a typical profile plot is shown in Fig. 1. As $\langle r_A \rangle$ increases, the cell volume rises and the orthorhombicity $(a - b)/(a + b)$ decreases smoothly (Fig. 2). The Cu–O bonds are under compression and the A–O bonds are under

TABLE 3
Results of Physical Measurements on A_2CuO_4 Samples 4–7: T_c (by ac susceptibility and resistivity measurements), F, ρ_{res}, S (290), and Hole Concentration, p

Sample no.	$\langle r_A \rangle$ (Å)	Oxygen content	T_c (K) (ACS)	F (%) at 5 K	T_c (K) (resistivity)	ρ_{res} (mΩ cm)	$S(290)$ ($\mu V K^{-1}$)	p
4	1.206	3.97(5)	—	—	6.7	0.55	28.7(5)	0.145
5	1.212	3.96(8)	—	—	8.4	0.52	26.2(5)	0.152
6	1.218	3.94(6)	21	4.7	18.1	0.27	25.0(5)	0.154
7	1.223	4.05(8)	20	6.2	19.0	0.15	44.6(5)	0.124

tension in the T structure, so that increasing $\langle r_A \rangle$ reduces both of these strains, decreasing the tilting of the CuO_6 octahedra and the cell orthorhombicity, ultimately resulting in a transition to the tetragonal structure for $\langle r_A \rangle \approx 1.223$ Å ($t = 0.87$).

b. Physical Properties

The physical properties of the single T phase samples 4–7 were investigated. Thermogravimetric analyses show that all four samples are oxygen stoichiometric within error, so the nominal hole doping level is fixed by the A cation compositions at 0.15 holes per Cu atom. Figure 3 shows the AC susceptibility curves for these samples. Samples 6 and 7 exhibit clear superconducting transitions with appreciable diamagnetic fractions at 5 K characteristic of bulk superconductivity, sample 4 shows a very small downturn around 10 K (see inset), and sample 5 shows no evidence of a diamagnetic transition. Four-probe electrical resistivity data (Fig. 4) show transitions for all four samples, suggesting that there are superconducting pathways percolating through samples 4 and 5, although bulk superconductivity is not observed by magnetic measurements. This is apparently at odds with previous results for a sample with similar $\langle r_A \rangle$ (= 1.212 Å) and σ^2 (= 0.019 Å^2) to sample 5 (5, 6). This sample had a magnetic T_c of 23 K and a fractional diamagnetism of $F = 4\%$ at 5 K, after annealing under 550 atm oxygen pressure, whereas the present samples were treated only under 1 atm oxygen pressure. It is clear that high-pressure annealing improves the superconducting properties of $(Ln^{3+}_{1-x}M^{2+}_x)_2CuO_4$ materials, principally by making the samples less granular.

All of the samples 4–7 show resistive upturns on cooling toward T_c, characteristic of underdoped cuprates, and the effect becomes less pronounced as $\langle r_A \rangle$ decreases. Values for the zero resistance T_c and the residual resistance extrapolated from the high-temperature linear regime to $T = 0$, ρ_{res}, were taken from these measurements and are given in Table 3. The ambient temperature thermoelectric power $S(290)$ is known to correlate with hole concentration p in systems such as $La_{2-x}Sr_x CuO_4$ and this correlation was used to estimate the p values shown in Table 3 which give a good measure of relative hole doping although the absolute accuracy is not as good. The value for sample 7 is clearly anomalous; the reason for this is not clear although

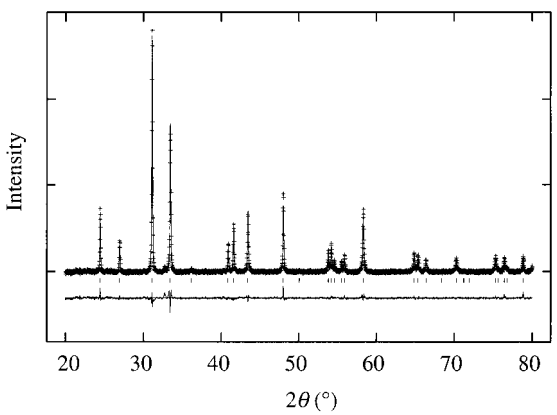

FIG. 1. Observed, calculated, and difference 290 K X-ray diffraction profiles for $(La_{0.925}Ca_{0.037}Sr_{0.008}Ba_{0.030})_2CuO_4$ (sample 7).

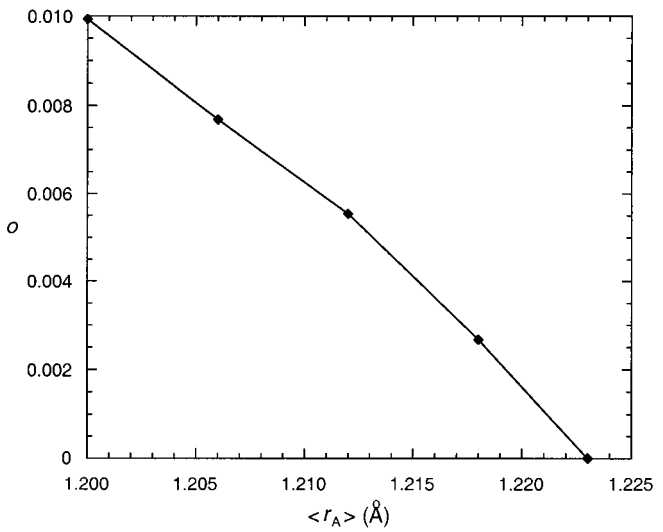

FIG. 2. Variation of orthorhombicity (o) with $\langle r_A \rangle$ for the T type phases in samples 3–7.

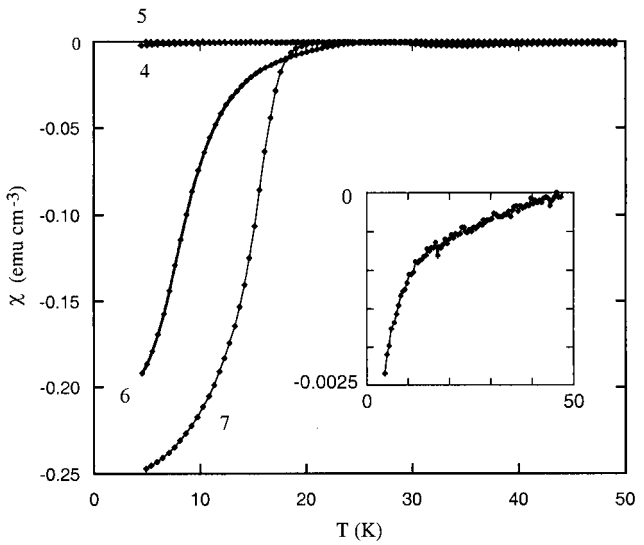

FIG. 3. Alternating current magnetic susceptibility data for samples 4–7. The inset shows the weak diamagnetism of sample 4.

we note that a sample of the same composition prepared in a previous study (of σ^2 effects at a constant $\langle r_A \rangle = 1.223$ Å (6)) had a T_c of 25 K which is more in keeping with the T_c trend for samples 3–6.

Despite some anomalies in the physical properties of sample 7, trends in the data in Table 3 are apparent. As $\langle r_A \rangle$ decreases at constant σ^2, T_c falls, ρ_{res} increases, and (excepting sample 7) $S(290)$ increases slightly. These changes are all consistent with a slight reduction in the free hole concentration in the normal state, the magnitude of which can be seen from the estimates of p in Table 3. A corresponding fall in the superfluid density below T_c is evidenced by the decrease in the fractional diamagnetism of the samples (and hence an increase in the penetration depth).

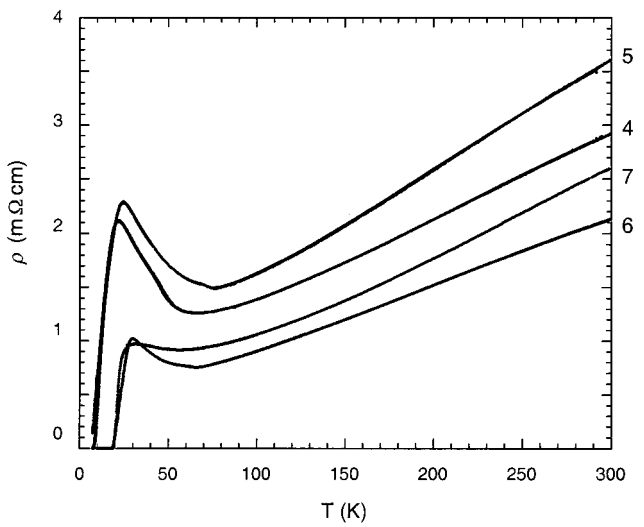

FIG. 4. Resistivity data for samples 4–7.

The above trends in physical properties with decreasing $\langle r_A \rangle$ at constant σ^2 are the same are those previously observed in $Ln^{3+}_{1.85}M^{2+}_{0.15}CuO_4$ materials with increasing σ^2 at constant $\langle r_A \rangle$ (6). The trends suggest that an increasing proportion of the current carrying holes is trapped as $\langle r_A \rangle$ decreases or σ^2 increases. This is in keeping with a simple empirical model for the effects of A cation size distributions proposed previously (5, 16), in which it is proposed that the temperatures of electronic transitions such as T_c in perovskite-type compounds decrease linearly with σ^2 at constant $\langle r_A \rangle$, and with $(r^0_A - \langle r_A \rangle)^2$ at constant σ^2 (r^0_A is the A cation radius that gives a tolerance factor of $t = 1$). However, the range of $\langle r_A \rangle$ over which the T type phase exists is too narrow to enable the latter quadratic function to be tested quantitatively here.

CONCLUSIONS

This study shows that true effects of varying tolerance factor t in doped perovskites such as the $(Ln^{3+}_{1-x}M^{2+}_x)_2CuO_4$ superconductors can be measured by fixing the size variance σ^2. This is achieved using mixtures of several cations such as those in Table 1 to give the desired size distribution and average charge. This approximation works well provided a single homogenous phase is synthesized, but when a mixture of phases results, as for samples 1 and 2, then the assemblage is a function of the proportions of individual cations rather than the statistics of the total distribution.

The qualitative results are in agreement with many earlier studies of $(Ln^{3+}_{1-x}M^{2+}_x)_2CuO_4$ superconductors, e.g., Ref. (1), as increasing the Cu–O–Cu bond angles toward 180° is known to enhance superconductivity (17). The structure type changes from the T′ to the T type with increasing t, at $t = 0.86$ for the fixed values of $x = 0.075$ and $\sigma^2 = 0.002$ Å^2 used here. The available A cations only enable T-type structures to be prepared up to $t = 0.87$; however, large changes in structure and property occur over the range $t =$ 0.865–0.871 studied for samples 4–7. The structure changes from orthorhombic to tetragonal, and the superconducting properties and normal state transport parameters all evidence a significant decrease in carrier trapping as t increases over this small range. These changes are the same as those previously observed when σ^2 is increased at constant t (5), although the rates of change were found to depend strongly on the value of t, and it is probable that different fixed σ^2 values will give different rates of change of property with t (all at constant x). Ultimately, this method of parameterization can be used to construct a four-dimensional phase diagram using T, x, t or $\langle r_A \rangle$, and σ^2 as variables to display the structure types and physical properties of all $(Ln^{3+}_{1-x}M^{2+}_x)_2CuO_4$ materials.

ACKNOWLEDGMENTS

We thank Dr. J. R. Cooper and Mr. S. F. W. R. Rycroft for help with transport measurements and EPSRC for support for J.A.M.

REFERENCES

1. A. Manthiram and J. B. Goodenough, *J. Solid State Chem.* **87,** 402 (1990).
2. J. B. Torrance, Y. Tokura, A. I. Nazzal, A. Bezinge, T. C. Huang, and S. S. P. Parkin, *Phys. Rev. Lett*. **61,** 1127 (1988).
3. D. M. Paul, G. Balakrishnan, N. R. Bernhoeft, W. I. F. David, and W. T. A. Harrision, *Phys. Rev. Lett*. **58,** 1979 (1987).
4. J. D. Axe, A. H. Moudden, D. Hohlwein, D. E. Cox, K. M. Mohanty, A. R. Moodenbaugh, and Y. W. Xu, *Phys. Rev. Lett*. **62,** 2751 (1989).
5. J. P. Attfield, A. L. Kharlanov, and J. A. McAllister, *Nature* **394,** 157 (1998).
6. J. A. McAllister and J. P. Attfield, *Phys. Rev. Lett*. **83,** 3289 (1999).
7. J. P. Attfield, A. L. Kharlanov, J. A. McAllister, and L. M. Rodriguez-Martinez, *Mater. Res. Soc. Symp. Proc*. **547,** 15 (1999).
8. R. D. Shannon, *Acta Crystallogr. A* **32,** 751 (1976).
9. A. C. Larson and R. B. Von Dreele, *Los Alamos National Laboratory Rep.* **LA-UR-86-748,** 1987.
10. S. D. Obertelli, J. R. Cooper, and J. L. Tallon, US Patent 5,619,141 (08/04/97).
11. *S*(290) v hole concentration data supplied by Dr. J. R. Cooper and C. Le Borngе.
12. Y. Tokura, H. Takagi, and S. Uchida, *Nature* **337,** 345 (1989).
13. H. Sawa, S. Suzuki, M. Watanabe, J. Akimitsu, H. Matsubara, H. Watabe, S. Uchida, K. Kokusho, H. Asano, F. Izumi, and E. Takayama-Muromachi, *Nature* **337,** 347 (1989).
14. A. R. Moodenbaugh, R. L. Sabatini, Y. W. Xu, J. Ochab, and J. G. Huber, *Physica C* **198,** 103 (1992).
15. H. Deng, C. Don, H. Chen, F. Wu, S. L. Jia, J. C. Shen, and Z. X. Zhao, *Physica C* **313** 285 (1999).
16. J. P. Attfield, *Chem. Mater*. **10,** 3239 (1998).
17. B. Dabrowski, Z. Wang, K. Rogachi, J. D. Jorgensen, R. L. Hitterman, J. L. Wagner, B. A. Hunter, P. G. Radaelli, and D. G. Hinks, *Phys. Rev. Lett*. **76,** 1348 (1996).